# The two annual northward jumps of the West Pacific Subtropical High and their relationship with summer rainfall in Eastern China under global warming*

Ye Tian-Shu(叶天舒), Zhi Rong(支 蓉)†, Zhao Jun-Hu(赵俊虎), and Gong Zhi-Qiang(龚志强)

*College of Atmospheric Sciences, Lanzhou University, Lanzhou* 730000, *China*

(Received 27 December 2013; revised manuscript received 16 February 2014; published online 20 April 2014)

The two northward jumps of summer West Pacific Subtropical High (WPSH) are defined based on the pentad-scale ridge data of the WPSH ridge in 1951 to 2012. The times of the northward jumps are found to have obvious inter-annual and decadal characteristics, i.e., the occurrence of the first northward jump of WPSH shows a "consistently early–consistently late" decadal pattern, with the transition around 1980; the occurrence of the second northward jump of WPSH shows a "consistently late–consistently early–consistently late" decadal pattern, with the transitions about 1955 and 1978, respectively, which is consistent with global warming. In the meantime, the times of the two northward jumps not only have a good correspondence to the beginning and ending dates of the rainy season, but also greatly influence the position of the main rain belt in Eastern China. When the first northward jump occurs early, the main rain belt is located from just north of 30° N to the south of North China, while the opposite situation appears when the first jump occurs late. When the second jump occurs early, more rain falls over North China and South China, but less falls in the Yangtze River region, while the opposite situation appears when the second jump occurs late. In the four cases when abnormalities occur in the same year as early or late northward jumps, the position of the main rain belt can be considered as a superposition of isolated abnormal effects of the two northward jumps. Moreover, the prophase and synchronous forces of the sea surface temperature in the Pacific has great influence on the times of the northward jumps, and the driving forces of the two jumps differ.

**Keywords:** northward jumps of WPSH, interannual variation, interdecadal variation, precipitation in Eastern China

**PACS:** 92.60.Ry **DOI:** 10.1088/1674-1056/23/6/069203

## 1. Introduction

The times of the two northward jumps of the West Pacific Subtropical High (WPSH) have an important impact on summer rainfall anomalies in Eastern China. Especially in the context of global warming, the variability of WPSH belonging to the East Asian monsoon is worthy of concern. Since the 1960s, many meteorologists have noticed the significant impact of West Pacific Subtropical High on China's climate, so that the anomaly causes of WPSH and its influence mechanism on China's summer climate are problems that concern Chinese meteorologists.[1–10] It was pointed out by Huang Shi-Song *et al.*[11] that the south–north changes in WPSH had slow and jumping movement characteristics, which was considered to be a global phenomenon. The seasonal variations in WPSH have a significant impact on short-term climatic anomalies, and its phased northward jump is directly related to both the rainy season and its position in Eastern China.[12–14] There are two obvious seasonal northward jumps of WPSH from early summer to mid-summer. On average, the first northward jump of WPSH occurs around mid-June. Then, the East Asian summer monsoon advances to the Yangtze River Basin, leading the Yangtze River–Huaihe River Basin into the rainy season. Around mid-July, the second northward jump of WPSH occurs, and then the East Asian summer monsoon advances to North China, and the rainy season of the Yangtze River–Huaihe River Basin is ended, while North China enters its rainy season.[15,16] Therefore, the research on the times of the two northward jumps of WPSH is of great significance to studies of the rainfall in Eastern China.

At present, much authoritative research has been completed on the time and latitude of northward jumps of WPSH within the season. Using day-scale TBB data for describing WPSH, Zhang Qing-Yun *et al.*[15] learned through statistics that the first northward jump occurs in the second pentad of June from just south of 20° N to 23° N, and the second northward jump occurs in the fourth pentad of July from just south of 26° N to 35° N. Tao Shi-Yan *et al.*[16] indicated that, from the climate perspective, the northward jump to 25° N of the WPSH ridge occurs around June 18, and the other northward jump, to 30° N, occurs around July 10°. Zhu Qian-Gen *et al.*[17] also pointed out that about the middle of June, the first northward movement of the ridge occurs north of 20° N, between 20° N∼ 25° N, which is conducive to the stability of the rainy season in the Yangtze River–Huaihe River Basin. The second northward jump occurs in mid-July, quickly passing

*Project supported by the National Basic Research Program of China (Grant Nos. 2012CB955902 and 2013CB430204), the National Natural Science Foundation of China (Grant Nos. 41175067 and 41105055), and the Special Scientific Research Fund of Public Welfare Profession of China (Grant No. GYHY201306021).

†Corresponding author. E-mail: z_rongphy@cma.gov.cn

© 2014 Chinese Physical Society and IOP Publishing Ltd 

25° N, leading to the termination of the Yangtze River–Huaihe River Basin rainy season and the start of the rainy season in North China. The above research only discusses the time and latitude of the two seasonal northward jumps of WPSH in a representative year. But, currently, the quantitative determination of northward ridge jump is lacking a workable calculation method. We thought that it is necessary to establish a relatively long time series of two northward jumps. After which, the work about the evolutionary characteristics of WPSH on scales of climatology and weather could be carried out, thus the quantitative relationship between WPSH and summer rainfall could be explored. In addition, the quantitative description of the time of two northward jumps of WPSH in the short-term climate prediction business is precisely the problem forecasters are most concerned about. Moreover, following global warming in the late 1970s, global ocean–atmosphere coupling system has also undergone a significant decadal change, when the East Asian summer monsoon circulation was weakened, while the WPSH as an important member of the East Asian summer monsoon was significantly enhanced southerly.[18–21] In this context, rare research was conducted on whether new changes occur to the inter-annual and decadal evolutionary characteristics of two northward jumps of WPSH. This paper attempts to find a new way to analyze and explain the reason for rainfall change.

To more realistically and quantitatively analyze the time of the two northward jumps of WPSH in summer and to find whether new changes occurred in the late 1970s, the pentad-scale ridge data of WPSH from 1951 to 2012 were used in this study to define the time of the two northward jumps. Their inter-annual and decadal evolutionary characteristics were analyzed as well as their relationship with summer rainfall in Eastern China. Important factors of the northward jumps of WPSH were revealed, which provide certain references for short-term climate prediction.

## 2. Data and method

### 2.1. Data

The data used in this study include: NCEP/NCAR daily wind field and monthly height field reanalysis data with horizontal resolution of $2.5^\circ \times 2.5^\circ$, monthly sea surface temperature field reanalysis data with horizontal resolution of $2^\circ \times 2^\circ$, and the monthly average rainfall data and monitoring data of the rainy season from 160 Chinese Stations from 1951 to 2012, provided by the National Climate Center (NCC).

### 2.2. Method

First, the daily ridge positions from May to October in 1951∼2012 were calculated in this study,[22] and then processed into pentad data (25–60 pentads). The processing method was as follows: the first five pentads of each month from May to October have five days for each pentad, and the sixth pentad is set from the 26th day to the last day of each month, in which the sixth pentads of May, July, August, and October are set to be six days, and those of June and September are set to be five days. The ridge position of a certain pentad is the sum of daily ridge positions divided by the number of days in the pentad. The following studies are based on pentad-scale ridge positions.

## 3. Definition of the times of the two northward jumps

Previous studies have shown that global climate and WPSH underwent a significant decadal change in the late 1970s.[18–21] Accordingly, the period of 1951–2012 was divided into two intervals; that is, 1951–1980 and 1981–2012. In order to more intuitively reveal the changes in WPSH ridge for each pentad in different intervals, the ridge position data of WPSH for each pentad from May to October in 62 years (25–60 pentads) are used herein to obtain the pentad average in different intervals, respectively. The results are shown in Fig. 1. It can be seen from Fig. 1 that the pentad ridge values of WPSH from 1951 to 1980 were basically higher than those from 1981 to 2012; that is, the overall positions of WPSH ridge were northerly prior to the 1980s, and the average ridge position was 22.5° N, 26.8° N, and 28.8° N from June to August, respectively, while the overall positions of WPSH ridge were southerly before the 1980s, and the average monthly ridge positions were 21.3° N, 26.2° N, and 28.3° N from June to August, respectively. In addition, from the 25th pentad to 31st pentad, the positions of the WPSH ridge were basically stable at 17° N ∼ 19° N (Area *A* in Fig. 1). From the 32nd pentad (the second pentad in June), the first northward jump of the WPSH ridge occurred over 20° N, then a stable region was entered at 23° N ∼ 25° N from the 35th pentad (Area *B* in Fig. 1), which was maintained in this region for about five pentads. The WPSH ridge jumped over 26° N at the 40th pentad (the 4th pentad in July); that is, the second northward jump of the WPSH ridge occurred, and it quickly entered another stable region at 28° N ∼ 31° N (Area *C* in Fig. 1), which was maintained for about six pentads. Subsequently, the WPSH ridge moved southward slowly after the 47th pentad (the 5th pentad in August). Thus, the average ridge positions were 20° N and 26° N, corresponding to the two northward jumps of WPSH, respectively.

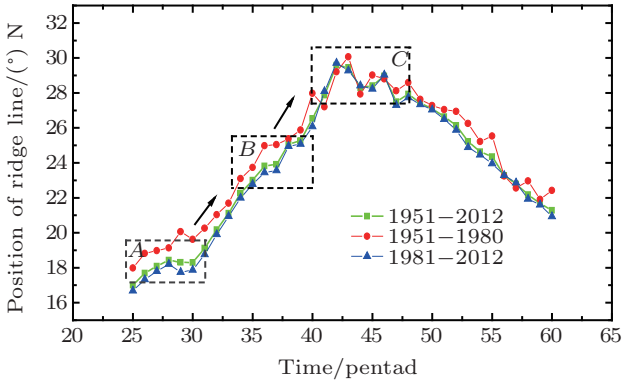



**Fig. 1.** (color online) Average position of ridge line of WPSH in different intervals.

Taking into account the great seasonal fluctuations of pentad ridge of WPSH and different degrees of drop in the ridge jumping over 20° N (26° N), the times of the two northward jumps are defined as follows: since the pentad for the first northward jump of WPSH ridge over 20° N (26° N), if the ridge is also located to the north of 20° N (26° N) in the next two pentads, then the pentad for the first northward jump over 20° N (26° N) is defined as the time of the first (second) northward jump; or in the case that the ridge is located to the north of 20° N (26° N) in the second pentad, if the ridge is not located to the north of 20° N (26° N), but located to the north of 19° N (25° N) in the third pentad, then the time of the first northward jump over 20° N (26° N) is defined as the time of the first (second) northward jump. According to the above definition, the time of the two northward jumps of WPSH from 1951 to 2012 was calculated (Table 1).

**Table 1.** Time of the two northward jumps form 1951 to 2012 (pentad).

| Year | First northward jump | Second northward jump | Year | First northward jump | Second northward jump | Year | First northward jump | Second northward jump |
|---|---|---|---|---|---|---|---|---|
| 1951 | 32 | 41 | 1972 | 33 | 38 | 1993 | 36 | 47 |
| 1952 | 31 | 45 | 1973 | 36 | 38 | 1994 | 34 | 37 |
| 1953 | 31 | 44 | 1974 | 27 | 41 | 1995 | 30 | 41 |
| 1954 | 27 | 43 | 1975 | 32 | 37 | 1996 | 32 | 40 |
| 1955 | 31 | 35 | 1976 | 32 | 40 | 1997 | 34 | 46 |
| 1956 | 27 | 37 | 1977 | 32 | 40 | 1998 | 34 | 51 |
| 1957 | 33 | 45 | 1978 | 32 | 38 | 1999 | 29 | 41 |
| 1958 | 33 | 39 | 1979 | 33 | 41 | 2000 | 33 | 40 |
| 1959 | 34 | 39 | 1980 | 31 | 50 | 2001 | 34 | 37 |
| 1960 | 29 | 39 | 1981 | 33 | 38 | 2002 | 34 | 41 |
| 1961 | 26 | 35 | 1982 | 38 | 42 | 2003 | 34 | 46 |
| 1962 | 27 | 41 | 1983 | 34 | 43 | 2004 | 35 | 40 |
| 1963 | 27 | 39 | 1984 | 35 | 35 | 2005 | 35 | 44 |
| 1964 | 34 | 40 | 1985 | 33 | 41 | 2006 | 34 | 42 |
| 1965 | 28 | 45 | 1986 | 34 | 48 | 2007 | 34 | 42 |
| 1966 | 35 | 39 | 1987 | 36 | 44 | 2008 | 32 | 41 |
| 1967 | 35 | 40 | 1988 | 31 | 42 | 2009 | 36 | 38 |
| 1968 | 34 | 44 | 1989 | 32 | 39 | 2010 | 38 | 40 |
| 1969 | 35 | 40 | 1990 | 33 | 40 | 2011 | 32 | 46 |
| 1970 | 33 | 41 | 1991 | 31 | 40 | 2012 | 34 | 40 |
| 1971 | 29 | 37 | 1992 | 38 | 41 | | | |

## 4. Inter-annual and decadal evolutionary characteristics of the time of the two northward jumps of WPSH

It can be seen from the departure accumulation (blue curve) in Fig. 2 that the times of the two northward jumps of WPSH have obvious inter-annual and decadal evolutionary characteristics. When the curve continues to drop (rise), it means the time of northward jump is consistently early (late). The time of the first northward jump of WPSH ridge experienced decadal change characteristics as "consistently early–consistently late" (Fig. 2(a)). The time of the first northward jump was consistently early before 1980 with an average northward jump time of the 31.3rd pentad (Table 2); that is, the early stage. Subsequently, the northward jump time was consistently late with an average northward jump time of the 33.8th pentad; that is, the late stage. In order to test whether the difference between the early stage (1951–1980) and late stage (1981–2012) is significant or not, a $t$ test was carried out on the original sequence of the first northward jump time, and the $t$ value was 3.93, passing the significance level test of

$\alpha = 0.001$. The time of the second northward jump of subtropical also has significant decadal changes (Fig. 2(b)), experiencing a decadal evolution as "consistently late–consistently early–consistently late." Before 1955, the second northward jump had the average time of the 43.3rd pentad, shown as the late stage. From 1955 to 1978, the average time was the 39.5th pentad, shown as the early stage. Since 1979 till now, the average time was the 41.9th pentad, shown as the late stage. The $t$ test value of the original sequence for the second northward jump time was 4.19 and 3.01 at the above two turning time points respectively, passing the significance level test of $\alpha = 0.01$.

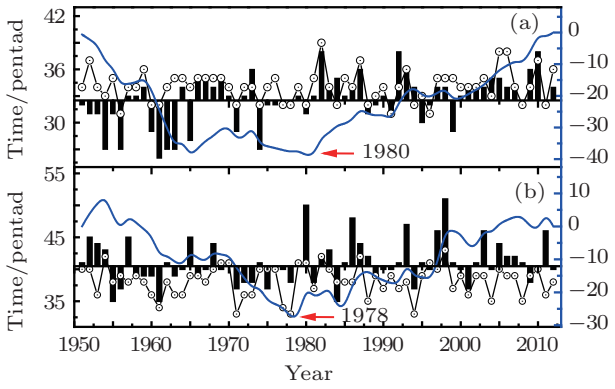



**Fig. 2.** (color online) Time series of northward jump times (column, units: pentad), their departure accumulation (blue curve) and beginning/end time of Meiyu (closed circle curve, units: pentad). (a) Time of the first northward jump, its departure accumulation and the beginning time of Meiyu; (b) time of the second northward jump, its departure accumulation and the end time of Meiyu.

**Table 2.** Average time of northward jumps time in different intervals and their significance test.

| | | 1951∼1980 | | 1981∼2012 |
|---|---|---|---|---|
| First northward jump | average time/pentad | 31.3 | | 33.8 |
| | $t$ testing value | | 3.93** | |
| | | 1951∼1954 | 1955∼1978 | 1979∼2012 |
| Second northward jump | average time/pentad | 43.3 | 39.5 | 41.9 |
| | $t$ testing value | 4.19** | 3.01* | |

Note: Superscripted $*$ and $**$ mean passing the significance level test of $\alpha = 0.05$ and $\alpha = 0.01$, respectively.

The standard deviation $\sigma$ of the times of the two northward jumps of WPSH ridge were 2.91 pentads and 3.16 pentads, respectively. The anomalous series of northward jump times is denoted as $X$. If the anomaly value of a certain year is $X_i \geq 0.5\sigma$, then this year is shown with a late northward jump; if $X_i \leq -0.5\sigma$, then this year is shown with an early northward jump. Accordingly, the years with early or late northward jumps of WPSH were obtained (Table 3). It can be seen from Table 3 that from 1951 to 1980, early northward jumps were more frequent than late jumps, while from 1981–2012, the late northward jumps were more frequent than early jumps; that is, northward jump times have very obvious inter-annual and decadal characteristics.

**Table 3.** The years with early or late northward jumps of different intervals.

| | Early stage | Late stage |
|---|---|---|
| Years of early first northward jump | 1952, 1953, 1954, 1955, 1956, 1960, 1961, 1962, 1963, 1965, 1971, 1974 | 1988, 1991, 1995, 1999 |
| Years of late first northward jump | 1959, 1964, 1966, 1967, 1968, 1969, 1973 | 1982, 1983, 1984, 1986, 1987, 1992, 1993, 1994, 1997, 1998, 2001, 2002, 2003, 2004, 2005, 2006, 2007, 2009, 2010, 2012 |
| Years of early second northward jump | 1955, 1956, 1958, 1959, 1960, 1961, 1963, 1966, 1971, 1972, 1973, 1975, 1978 | 1981, 1984, 1989, 1994, 2001, 2009 |
| Years of late second northward jump | 1957, 1965, 1968 | 1952, 1953, 1954, 1980, 1983, 1986, 1987, 1993, 1997, 1998, 2003, 2005, 2011 |

## 5. The relationship between northward jump time and summer rainfall in Eastern China

The seasonal activities of WPSH are closely related to the starting and ending time of the rainy season in different areas of Eastern China. The first northward jump of WPSH substantially corresponds to the beginning of Meiyu, and the second northward jump corresponds to the end of Meiyu and the start of rainy season in North China.[12–14] On this basis, the start and end date of Meiyu in the monitoring data of the rainy season provided by NCC were used for comparative analysis with the times of the two northward jumps

in this study, and annual corresponding situations are shown in Fig. 2. Due to the presence of non-Meiyu phenomena in the monitoring data, the start and end dates of Meiyu in non-Meiyu years were set (for a total of five non-Meiyu years) by the average start and end dates of Meiyu in the years that had Meiyu. Overall, the times of the two northward jumps of WPSH are basically consistent with the start and end dates of Meiyu. The correlation coefficients of the times of the two northward jumps to the start and end dates of Meiyu are 0.50 and 0.44, respectively, passing the significance level test of $\alpha = 0.001$. Moreover, the average start time of Meiyu is the 34th pentad, which is later than the time of the first northward jump of WPSH by two pentads, while the average end time of Meiyu is the 38th pentad, which is earlier than the time of the first northward jump of WPSH by two pentads. The "staggered" result between the times of northward jumps and the start and end times of rainy season is consistent with the research results of Xu Hai-Ming *et al.*[23] In the years of extremely early or late start and end times of Meiyu, the times of the two northward jumps also correspond well, e.g., 1956, 1982, 1987, 1991, 2005, 2006, and 2010 (Fig. 2(a)); 1954, 1961, 1971, 1982, 1978, 1994, and 1998 (Fig. 2(b)). In the 62-year scope of the study, the anomaly sign is consistent between the time of the first northward jump and the start time of Meiyu in 41 years, accounting for 66%; that is consistent in 47 years with the time of the second northward jump and the end time of Meiyu, accounting for 76% of all the years. However,

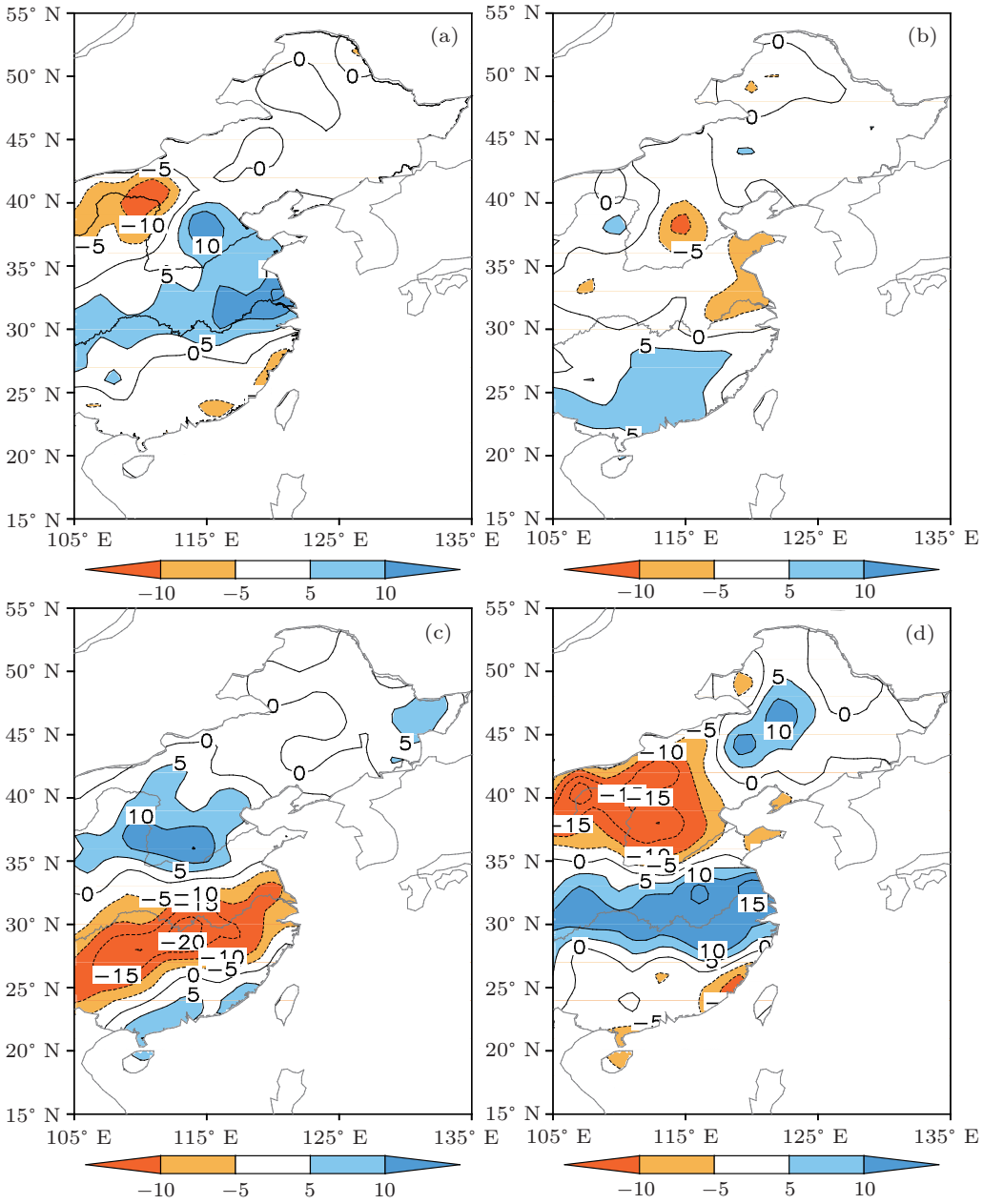



**Fig. 3.** (color online) The composition of summer rainfall anomalous percentages in the years of early or late northward jumps (%). Years of the first northward jump being (a) early and (b) late; years of the second northward jump being (c) early and (d) late.

for the years with the start and end times of Meiyu close to normal, an early or late anomaly occurs in the times of northward jumps of WPSH. The reason for such incomplete correspondence is that the start and end dates of Meiyu are not only influenced by the time of the northward jumps of the WPSH ridge. Moreover, the time interval between the two northward jumps of WPSH, that is, the correlation coefficient between the stability after the first northward jump and that of Meiyu is 0.32, also passed the significance level test of $\alpha = 0.001$.

The times of the two jumps of the ridge not only correspond with the occurrence times of the rainfall in Eastern China, but they also influence the spatial distribution of rainfall greatly. The composition of summer rainfall anomalous percentages in the years of early or late jumps of WPSH (Table 3) is shown in Fig. 3. If only the years for early first northward jumps (Fig. 3(a)), (generally bounded by 30° N (Yangtze River Basin)) are considered, the rainfall is less to the south of 30° N, but more from the north of 30° N to just south of North China. However, if only the years for late first northward jumps are considered, the opposite state is shown (Fig. 3(b)); that is, the rainfall is more to the south of 30° N, but less from the north of 30° N to just south of North China. It can be seen that the rainfall difference caused by the anomaly of

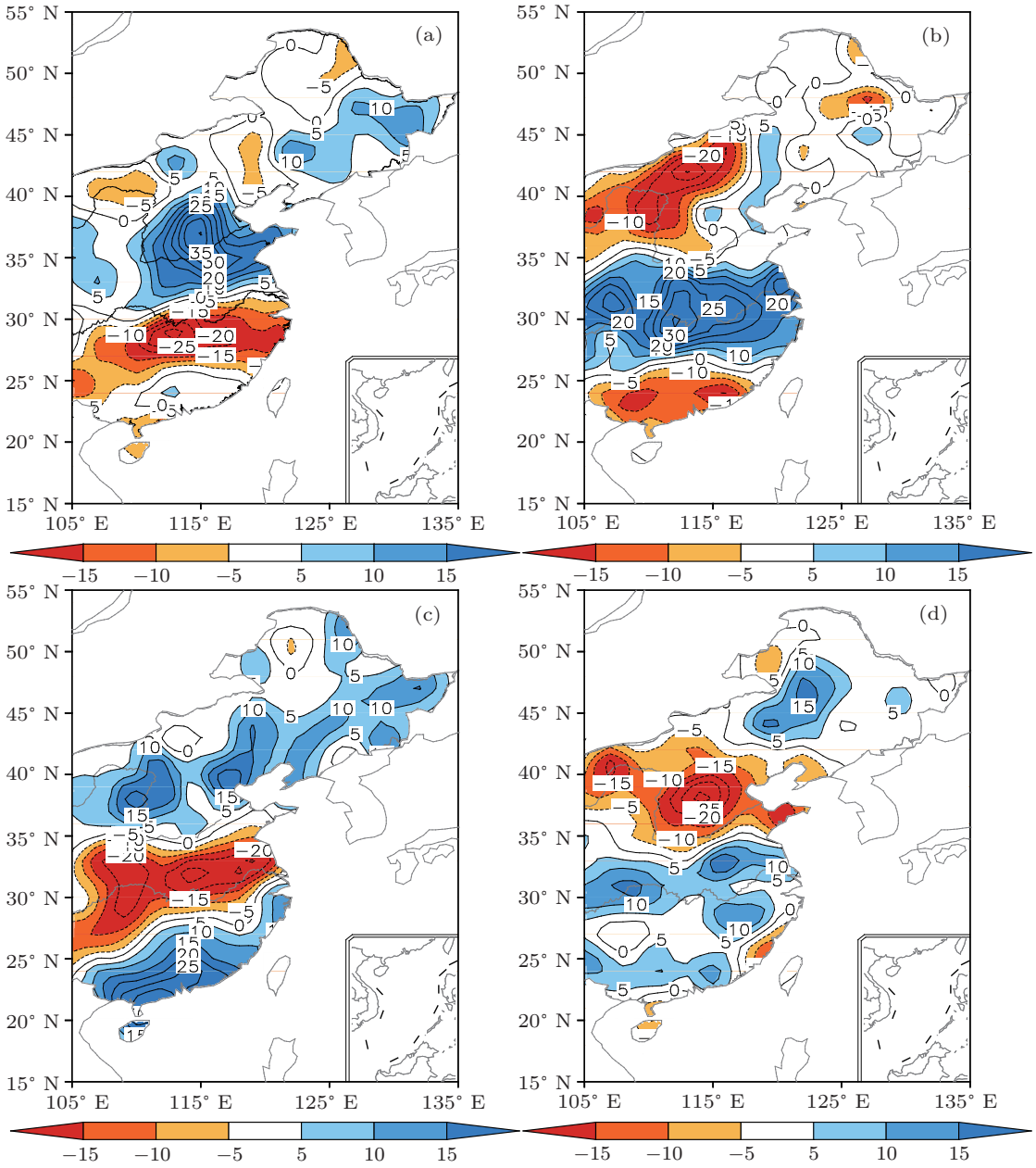



**Fig. 4.** (color online) The composition of summer rainfall anomaly percentages in different configurations of time of the two northward jumps (%). (a) The early occurrences of both northward jumps; (b) the early occurrences of the first jump when the second jump was late; (c) the late occurrences of the first jump when the second jump was late; (d) the late occurrences of both northward jumps.

the first northward jump mainly occurs in the north and south of Yangtze River Basin. Similarly, if only the years for early second northward jumps are considered, the more rain falls in North China, Hetao Region, and South China, but less in Yangtze River Basin (Fig. 3(c)). The situation is basically opposite in the years for late second northward jumps (Fig. 3(d)). It can be seen that, comparing the rainfall anomaly caused by the anomaly of the second northward jump with the first northward jump, the boundary of 30° N evolves into two boundaries; that is, 25° N and 35° N. Thus, the following question arises: What is the distribution of rainfall anomalies in the years with anomalous northward jumps?

The years with anomalies in the two northward jumps were screened in Table 3 for the composition of summer rainfall anomalous percentages, that is, the four situations, including the two jumps both being early, the first jump being early while the second jump was late, the first jump being late while the second jump was early, and the two jumps both being late. Figure 4 shows the anomalous distribution of summer rainfall in the four different configurations. Figure 4(a) indicates the composition of summer rainfall anomalous percentages in the years when the two jumps were both early. In this case, roughly bounded by 30° N, the main rain belt is located from just north of 30° N to North China and Northeast China, and less rain fell from just south of 30° N to South China. The combined effect is basically shown by the superposition of Figs. 3(a) and 3(c). When the first northward jump occurs early while the second jump occurs late, roughly bounded by 25° N and 35° N, the main rain belt is located between 25° N and 35° N, and the less rain falls in Hetao Region and central Inner Mongolia from the south of 25° N to the north of 35° N (Fig. 4(b)). The combined effect is basically shown as the superposition of Figs. 3(a) and (d). Figure 4(c) shows the rainfall anomaly distribution of the late occurrences of the first jump and the early occurrences of the second jump, such results are substantially contrary to Fig. 4(b). The combined effect is basically shown as the superposition of Figs. 3(b) and 3(c). Figure 4(d) shows the rainfall anomaly distribution in the late occurrences of both the two northward jumps. The difference in Fig. 4(a) is that the boundary of positive and negative anomaly moved around 35° N, and the rainfall anomaly percentage signs are opposite on the north and south sides of the boundary. The combined effect is basically shown as the superposition of Figs. 3(d) and 3(b). It can be seen that if the anomalies in the times of the two northward jumps are considered comprehensively, the results are generally similar to the superposition of two independent northward jumps, but also there is a slight difference.

## 6. The relationship between anomalous times of the two northward jumps and sea surface temperature anomalies, both prophase and synchronous

### 6.1. The relationship between the times of the two northward jumps and ENSO

The changes in north-south position of WPSH are not only the result of atmospheric internal dynamic process, but are also inseparable from the thermal conditions in the underlying surface of the ocean.[24–27] It can be seen from Figs. 5(a1)–(a3) and Figs. 5(c1)–(c3) that in the years when the first and second northward jumps were early, pre-winter central and eastern equatorial Pacific sea surface temperature anomaly (SSTA) show strong negative anomaly, which is in a strong La Niña stage. In the subsequent pre-spring and summer, the center intensity of maximum negative anomaly is weakened and retreated eastward, experiencing a La Niña weakening process. In addition, from the pre-winter to summer, the positive anomaly intensity and range of SSTA to the east of Japan as North Pacific mid-latitude are continuously increasing. However, the situation in the years of late northward jumps is opposite to the early years, showing an El Niño state (Figs. 5(b1)–5(b3)) and Figs. 5(d1)–(d3). Furthermore, there are also differences between the years when the two jumps were late. In the pre-winter of the years when the first jump was late (Figs. 5(b1)), the equatorial middle-eastern Pacific shows a strong El Niño state, but it gradually weakens until the demise in the subsequent spring and summer (Figs. 5(b2)–5(b3)). The SSTA to the east of Japan changes from positive anomaly to negative anomaly, while the situation in the years when the second jump was late (Figs. 5(d1)–(d3)) is opposite to the years when the first jump was late. From the pre-winter to summer, El Niño transforms from “developing” to intense. The SST in the sea to the east of Japan changes from positive anomaly to negative anomaly. It can be seen that the development process of sea surface temperatures (SST) from pre-winter to summer has a certain significance to predict the anomalies in the time of the following summer’s northward jumps of WPSH.

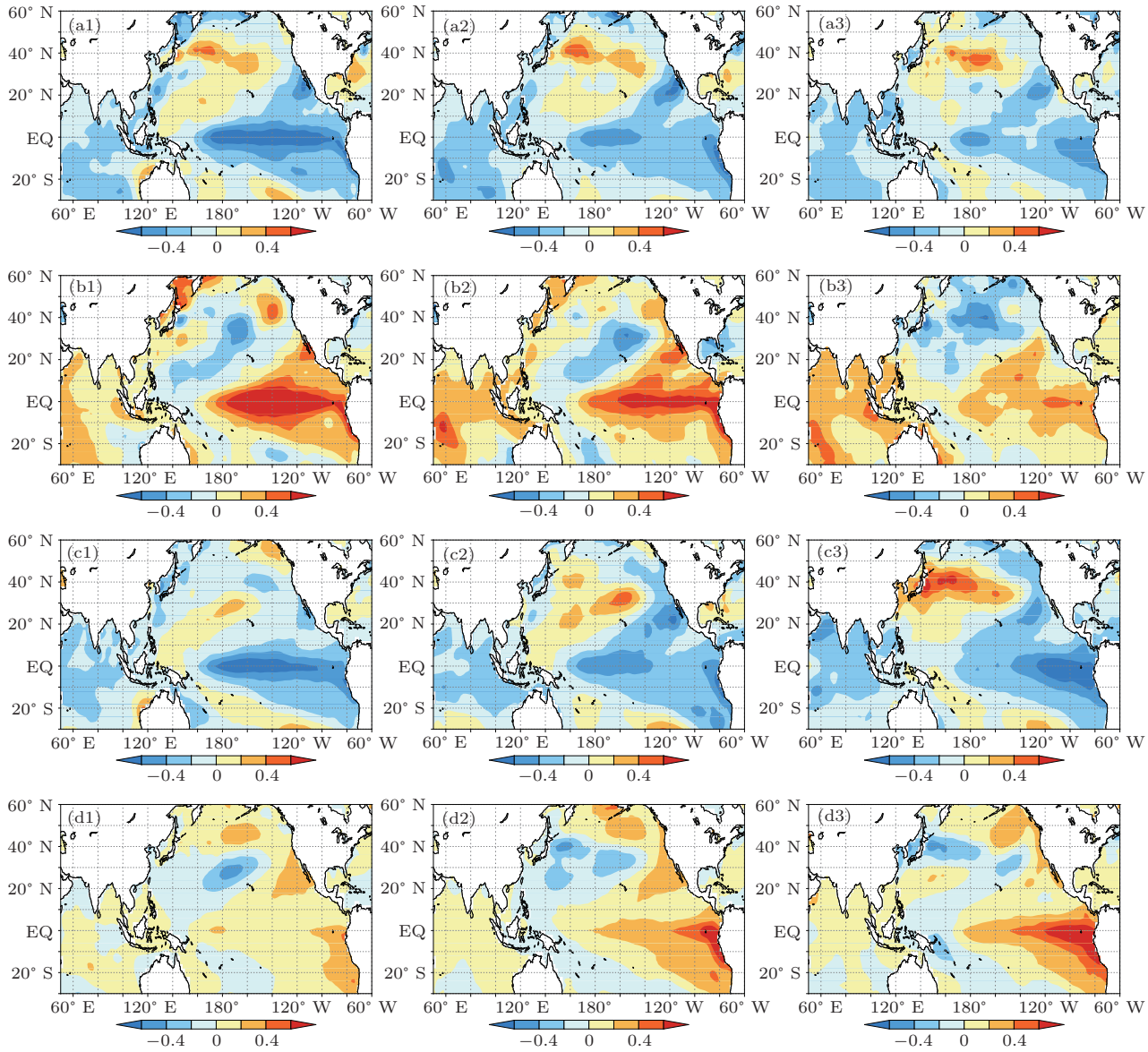



**Fig. 5.** (color online) The composition of SSTA in the years of early or late northward jumps. (°C) Years when the first jump was (a) early and (b) late; years when the second northward jump was (c) early and (d) late; (a1)–(d1) pre-winter; (a2)–(d2) spring; (a3)–(d3) summer.

### 6.2. The relationship between the times of the two northward jumps and different sea areas of El Niño

It can be seen from above that the time of the two northward jumps has a lot to do with ENSO, in the next section the correlation coefficients will be calculated between the time of the two northward jumps and indexes in different sea areas of Niño from January to December (Fig. 6). It can be seen from Fig. 6(a) that, overall, the correlation coefficients between the first jump and the indexes in every sea area of El Niño were all positive. As for the same sea area, the correlation coefficients before June (average time of first northward jump) were higher than after June, and it reached the maximum in April–May. Outside the correlation coefficient between the first northward jump and index in Niño1+2, the other peaks all passed the significance level test of $\alpha = 0.05$. Niño4 has the most months that pass the significance level test, and Niño1+2 has the least. The color from deep to shallow represents the geographic location of sea areas from east to west, respectively. We discovered that, outside October–November–December, the correlation coefficient was related to the geographic location, increasing gradually from east to west, for the same month increasing, for a given month, the correlation coefficient was smallest in Niño1+2, and largest in Niño4. It can be seen from Fig. 6(b) that the correlation coefficients between the second northward jump and indexes in every sea area of Niño were also all positive. As for the same sea area, the correlation coefficients before July (average time of second northward jump) were higher than after July, and it

also reached the maximum in April–May. The peaks all passed the significance level test of $\alpha = 0.05$. Unlike the first northward jump, Niño1+2 had the most months passed the significance level test, and Niño4 had the least. We discovered that, outside January–February–March and August, the correlation coefficient was related to the geographic location, decreasing gradually from east to west for a given month; that is, in a given month, the correlation coefficient was smallest in Niño4 and largest in Niño1+2, which is contrary to the case for the first jump.

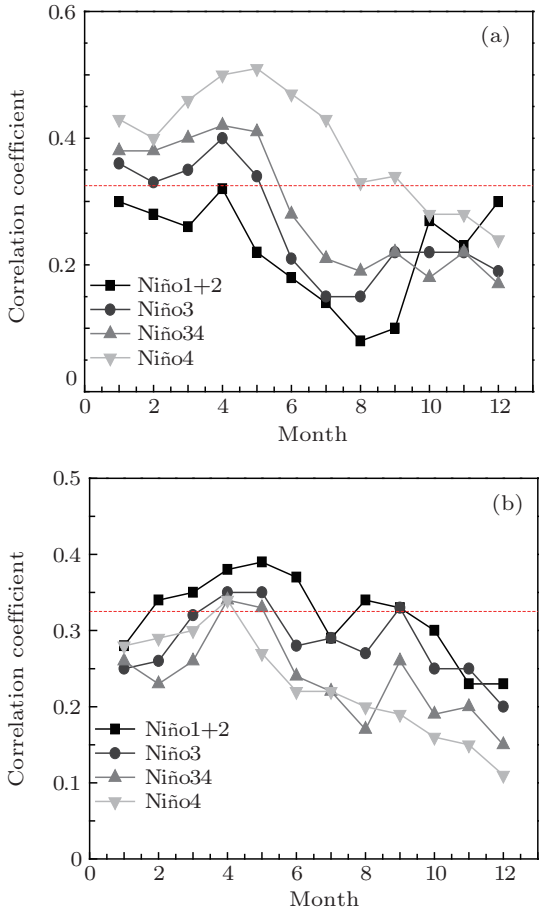



**Fig. 6.** Correlation coefficient between first northward jump (a), second northward jump (b) and indexes in different sea areas of El Niño from January to December. (Red dotted line means passing the significance level test of $\alpha = 0.05$.)

From the correlation, we can see that the correlation coefficients between the two jumps and the indexes in every sea area of El Niño were all positive, and it was higher before a northward jump than afterward, and it reached the maximum in April–May. However, significant differences still exist: for the first jump, the correlation coefficients increase gradually from east to west, but for the second jump, the correlation coefficients decrease gradually from east to west. These gradients illustrate that the driving forces are different, and the account of the mechanisms has to be improved in subsequent research.

## 7. Conclusion and discussion

Due to global warming in the late 1970s, a global decadal adjustment occurred to the air–sea coupling system in east Asia. The 62-year pentad-scale WPSH ridge data from 1951 to 2012 were used to define the calculation method of the time of the two northward jumps in this study. They were also used to analyze the inter-annual and decadal evolutionary characteristics and their relationship with summer rainfall before and after the onset of global warming. The specific conclusions are shown as follows:

(i) According to decadal turning characteristics of the time of the two northward jumps from 1951 to 2012, the time of the first northward jump can be roughly divided into three stages, that is, "consistently early–consistently late", and the transition was around 1980; "consistently late–consistently early–consistently late" decadal fluctuations were found in the times of the second northward jump, and the transitions were around 1955 and 1978.

(ii) The times of the two northward jumps of the WPSH ridge influence the rainfall in Eastern China greatly. In the early time of the first northward jump, the main rain belt in Eastern China is located to the north of 30° N from the Yangtze River Basin to southern North China, while less rain falls to the south of 30° N; the opposite situation exists whenever the first northward jump is late. When the second jump is early, more of Eastern China's rain falls in South China and North China than in the Yangtze River Basin; the opposite situation exists in the years when the second jump is late.

(iii) In the years when both the northward jumps are early, the main rain belt is located in the north, ranging from just north of 30° N to southern North China, while less rain falls in the range from just south of 30° N to South China. The opposite situation exists in the years when both jumps are late. If the first jump is early and the second jump is late, the main rain belt of Eastern China is located between 25° N and 35° N, while less rain falls in the Hetao Region and central Inner Mongolia from just south of 25° N to just north of 35° N; the opposite situation exists if the first jump is late and the second jump is early. Moreover, these four cases can be seen as the superposition of separate anomalous effects of the two northward jumps.

(iv) The early or late occurrences of the two northward jumps of WPSH are also closely related to the SST forces at

play in the preceding months. From the pre-winter to summer of the years when the first and second jumps are both early, the equatorial mid-eastern Pacific La Niña is weakened from strong intensity. From the pre-winter to summer of the late years for the first and second northward jumps, El Niño phenomenon occurs. The difference is that in the "late" years for the first jump, El Niño is weakened to a demise, while in the "late" years for the second jump, El Niño evolves from early development to strong intensity.

(v) The correlation coefficients between the two northward jumps and the indexes in every sea area of El Niño were all positive, and it reached the maximum in April–May. For the first jump, the correlation coefficients increase gradually from east to west, but for the second jump, the correlation coefficients decrease gradually from east to west.

Due to limited space, the two northward jumps of WPSH were defined to briefly analyze the inter-annual and decadal evolutionary characteristics of the time of the two northward jumps of summer WPSH in the past 62 years, as well as their impacts on the summer rainfall in Eastern China. With the application of a method combining dynamics and statistics in recent years, short-term climate prediction, especially rainfall prediction techniques, has improved to a certain extent,[28–31] but limitations still exist in prediction.[32] Considering the anomaly in the times of the northward jumps of WPSH may improve prediction even more. In the present study, the times of northward jump of WPSH were defined, and the effects of the times of the northward jumps on summer rainfall anomalies were discussed, providing certain ideas for short-term climate prediction with consideration of the times of these jumps. The climate system is a giant, complex, highly nonlinear, non-scale, multi-layered, and force-dissipative system that changes through a non-stationary process.[33–43] Methods for predicting the times of the two northward jumps will be discussed in the next step of our research.

## References


[1] Tao S Y and Xu S Y 1962 *Acta Meteorol. Sin.* **32** 1 (in Chinese)
[2] Sha W Y and Guo Q Y 1998 *J. Appl. Meteorol.* **9** 31 (in Chinese)
[3] Zhang Q Y and Tao S Y 2003 *J. Atmos. Sci.* **27** 369 (in Chinese)
[4] Lian Y, Shen B Z, Gao Z T, An G and Tang X L 2003 *Acta Meteorol. Sin.* **61** 548 (in Chinese)
[5] Fan K and Wang H J 2006 *J. Atmos. Sci.* **30** 402 (in Chinese)
[6] Wang H J 2010 *Adv. Earth. Sci.* **25** 643 (in Chinese)
[7] Feng G L, Yang H W, Zhang S X, Wang K and Shen B Z 2012 *J. Atmos. Sci.* **36** 1009 (in Chinese)
[8] Shen B Z, Zhang S X, Yang H W, Wang K and Feng G L 2012 *Acta Phys. Sin.* **61** 109202 (in Chinese)
[9] Yang J, Feng G L, Zhao J H and Zhang Z S 2012 *Acta Meteorol. Sin.* **70** 1032 (in Chinese)
[10] Zhao J H, Feng G L, Yang J, Zhi R and Wang Q G 2012 *Acta Meteorol. Sin.* **40** 1021 (in Chinese)
[11] Huang S S 1978 *J. Atmos. Sci.* **2** 160 (in Chinese)
[12] Liang J Y 1994 *J. Trop. Meteorol.* **10** 274 (in Chinese)
[13] Wei J, Yang H and Sun S Q 2004 *Acta Meteorol. Sin.* **62** 308 (in Chinese)
[14] Tan G R and Sun Z B 2004 *J. Trop. Meteorol.* **20** 206 (in Chinese)
[15] Zhang Q Y and Tao S Y 2000 *Acta Meteorol.* **57** 539 (in Chinese)
[16] Tao S Y and Wei J 2006 *J. Appl. Meteorol.* **17** 513 (in Chinese)
[17] Zhu Q G, Lin J R, Shou S W and Tang D S 2007 *Synoptic Meteorology Principle and Methods*, 4th edn. (Beijing: China Meteorological Press) pp. 354–367 (in Chinese)
[18] Wang H 2001 *Adv. Atmos. Sci.* **18** 376
[19] Xue F 2001 *Adv. Atmos. Sci.* **18** 567
[20] Gong D Y and He X Z 2002 *Acta Geograph. Sin*. **57** 185 (in Chinese)
[21] Xue F and Su T H 2009 *Prog. Nat. Sci.* **19** 421 (in Chinese)
[22] Liu Y Y, Li W J, Ai Y X and Li Q Q 2012 *J. Appl. Meteorol.* **23** 414 (in Chinese)
[23] Xu H M, He J H and Zhou B 2001 *J. Appl. Meteorol.* **12** 150 (in Chinese)
[24] Gong D Y and Wang S W 1998 *Acta Ocean. Sin.* **20** 44 (in Chinese)
[25] Yang Y W, Wu X X and Ai Y X 1998 *J. Appl. Meteorol*. **9** 90 (in Chinese)
[26] Wei W, Zhang R H and Wen M 2012 *J. Appl. Meteorol.* **23** 650 (in Chinese)
[27] Nitta T 1987 *J. Meteor. Soc. Jpn.* **65** 373
[28] Wang Q G, Feng G L, Zheng Z H and Zhi R 2011 *Chin. J. Atmos. Sci.* **35** 288 (in Chinese)
[29] Yang J, Wang Q G, Zhi R and Feng G L 2011 *Acta Phys. Sin.* **60** 029204 (in Chinese)
[30] Xiong K G, Feng G L, Huang J P and Chou J F 2012 *Acta Meteorol. Sin.* **70** 213 (in Chinese)
[31] Feng G L, Sun S P, Zhao J H and Zheng Z H 2013 *China Earth Sci.* **56** 1576
[32] Zhao J H, Feng G L , Wang Q G, Yang J and Gong Z Q 2011 *Chin. J. Atmos. Sci.* **35** 1071 (in Chinese)
[33] Feng G L, Dong W J, Gong Z Q, Hou W, Wan S Q and Zhi R 2006 *The Theory and Method about the Spatial and Temporal Distribution of the Observation Data's Nolinear* (Beijing: China Meteorological Press) p. 227 (in Chinese)
[34] Feng G L, Hou W and Dong W J 2006 *Acta Phys. Sin.* **55** 962 (in Chinese)
[35] Gong Z Q, Feng G L, Dong W J and Li J P 2006 *Acta Phys. Sin.* **55** 3181 (in Chinese)
[36] Feng G L, Dai X G, Wang A H and Chou J F 2001 *Acta Phys. Sin.* **50** 606 (in Chinese)
[37] Wang X J, Zhi R, He W P and Gong Z Q 2012 *Chin. Phys. B* **21** 029201
[38] Gong Z Q, Feng G L, Wan S Q and Li J P 2006 *Acta Phys. Sin*. **55** 477 (in Chinese)
[39] Feng G L, Dong W J, Jia X J and Cao H X 2002 *Acta Phys. Sin.* **51** 1181 (in Chinese)
[40] Huang J P, Yi Y H, Wang S W and Chou J F 1993 *Quart. J. Roy. Meteor. Soc.* **119** 547
[41] Huang J P and Yi Y H 1991 *Sci. China B* **34** 1246
[42] Zhang Z S, Gong Z Q, Zhi R, Feng G L and Hu J G 2011 *Chin. Phys. B* **20** 019201
[43] Gong Z Q, Wang X J, Zhi R and Feng A X 2011 *Chin. Phys. B* **20** 079201